

Hindawi Publishing Corporation International Journal of Distributed Sensor Networks Volume 2015, Article ID 738974, 12 pages http://dx.doi.org/10.1155/2015/738974

Research Article

Critical Density for Exposure-Path Prevention in Three-Dimensional Wireless Sensor Networks Using Percolation Theory

Guixia Kang, Xiaoshuang Liu, Ningbo Zhang, Yanyan Guo, and Fabrice Labeau

Key Laboratory of Universal Wireless Communication, Ministry of Education, Beijing University of Posts and Telecommunications, Beijing 100876, China

Correspondence should be addressed to Xiaoshuang Liu; lxs_55@163.com

Received 24 August 2014; Accepted 14 December 2014

Academic Editor: Eleana Asimakopoulou

Copyright © 2015 Guixia Kang et al. This is an open access article distributed under the Creative Commons Attribution License, which permits unrestricted use, distribution, and reproduction in any medium, provided the original work is properly cited.

To derive the critical density for exposure-path prevention in three-dimensional wireless sensor networks (3D WSNs), a bond-percolation-based scheme is proposed, which can generate the tighter lower and upper bounds of critical density. Firstly, the exposure-path prevention problem and system models based on Gaussian distribution are introduced in this paper. Then, according to percolation theory, we present a bond-percolation model to put this problem into a 3D uniform lattice. With this model, the lower and upper bounds of critical density for 3D WSNs are derived in the light of our scheme. Extensive simulations and contrast experiments also validate our developed models and evaluate the performance of the proposed schemes. Therefore, our scheme can be applied to determine a practically reliable density and detect intruders in sensor networks.

1. Introduction

Over the past decades, wireless sensor networks (WSNs) have represented one of the most outstanding technologies, and several research disciplines, such as communication protocols, and hardware platforms, have appeared to cover the special requirements of these systems. Many applications of WSNs need the intrusions being detected by sensor nodes in the interested region [1], like military applications, healthy environment monitoring, seism surveillance, and so on. The intrusion detection problem belongs to node coverage issue that is vital in the area of WSNs. Moreover, if nodes detect intrusion paths, the intrusions can be detected. Namely, coverage of intrusion paths has important influence in detecting intrusions.

Generally, coverage reflects QoS (quality of service) provided by sensor nodes of networks [2]. It creates collaborations among the nodes in covering an interested region for monitoring specific information. The researchers have studied the coverage problem from many different perspectives based on different requirements [3, 4]. As shown in the majority of references [2–4], if each point in the region

is sensed by at least one sensor node, this region is defined as covered region. However, if the objective of coverage is to detect moving targets or phenomena, the traditional full coverage model [2-4] may be unnecessary. Full coverage means that everywhere in the deployment area is covered by nodes, which is at the cost of resource wastes and high complexity [5]. But coverage for intrusion detection only needs partial coverage ensuring that no moving targets or phenomena can pass through the interested region without being detected [6]. If an intruder can traverse through the deployment area and the resulting path is not covered by nodes, we name the traversed path as the exposure path. It reflects the ability of intrusions moving through the deployed area [7]. Preventing the exposure paths belongs to the exposure-path prevention problem. On account of the full coverage, network coverage is rather poor if there exists an exposure path in WSNs [8]. Hence, this paper considers the problem of no exposure path in 3D WSNs.

To address the exposure-path problem, this paper adopts percolation theory [9–11] to compute the optimal density in order to make the probability of an exposure path existing converge to 0 and satisfy the minimum density of sensor

nodes. In [12], Broadbent and Hammersley first introduced percolation theory to model the disordered media and simulate the percolation process of immersed rocks. Since this theory reveals the vital relationships between probabilistic and topological characteristics of graphs, it is attractive to researchers [13] and has been used to study connectivity of WSNs [14–16]. In this paper, we exploit the percolation theory to obtain the optimal density for coverage inomnidirectional sensor networks.

On the basis of percolation theory [10, 13], if p is the average degree of connectivity between various subunits of some arbitrary system, there exists a percolation threshold, denoted by p_t . When $p \ge p_t$, there is no exposure path from one side to the other side of this system, and not vice versa. Deriving the critical density to achieve regional coverage for random network deployment process is a fundamentally important problem in the area of WSNs. Based on percolation theory, most existing studies [14–16] apply the continuumpercolation theory to derive the optimal density for coverage. However, the studies suffer from the loose lower and upper bounds of critical density and cannot be applied to determine a practically useful density for network deployment. In this paper, a bond-percolation scheme is proposed in 3D WSNs to conquer the above problem and make percolation theory more suitable for the exposure-path problem. We assume sensor nodes deployed under a 3D Gaussian process, and the rigorous derivation analyses and simulation results indicate that the proposed method can generate much tighter upper and lower bounds of critical density.

The remainder of our paper is structured as follows. Section 2 introduces the related works, and based on Gaussian distribution, Section 3 presents the system models and problem formulation about exposure-path prevention in 3D WSNs. Section 4 describes the bond-percolation theory to derive and analyze the optimal critical density for exposure-path problem. In addition, the mutual dependence among edges of the proposed scheme is dealt with in this section. In Section 5, extensive simulation results evaluate the models and schemes we proposed, and the last section concludes this paper.

2. Related Works

In this section, we introduce the related works of percolation theory and exposure-path problem in WSNs. Due to coverage of exposure paths belonging to barrier coverage, this section also presents recent results about barrier coverage.

The coverage of WSNs can be classified into three types: area coverage, barrier coverage, and point coverage in terms of the different covered objects [17]. Area coverage is full coverage, while barrier coverage and point coverage are partial coverage. Area coverage needs every point within the target area covered by at least one node [18]; barrier coverage measures the detection ability [19]; point coverage requires the coverage of several discrete targets [20]. In this paper, barrier coverage contains the mentioned exposure-path problem. Next, we introduce the related researches on exposure-path problem.

In [21], the authors provided formal yet intuitive formulations, established the complexity of the exposure-path problem and developed practical algorithms for exposure calculation. They also investigated the relationship and interplay of exposure problem with other fundamental wireless sensor network tasks and in particular with location discovery and deployment. After elucidating the importance of the exposure problem, Megerian et al. [22] formally defined exposure paths and studied exposure-path properties. Meanwhile, they developed an efficient-effective algorithm for exposure calculations in sensor networks, specifically for finding minimum exposure paths. Veltri et al. [23] proposed an efficient localized algorithm enabling a sensor network to determine its minimum exposure path. Theoretical highlight of this reference is the closed-form solution for minimum exposure in the presence of a single sensor node. Moreover, they introduced a new coverage problem, the maximum exposure path, which was proved NP-hard and could be resolved by heuristics to generate approximate solutions. The concept of information exposure was came up in [24], and an approximation algorithm was presented to solve the problem of finding the worst (best) information exposure path in WSNs. In [25, 26], an approximation algorithm was suggested by Djidjev to solve the minimum exposure-path problem and guaranteed the network performance. Ferrari and Foderaro [27] introduced an artificial-potential approach that designed the minimum exposure paths of multiple mobile objects (including sensor nodes) in dynamic networks. In addition, this approach can be used in heterogeneous wireless sensor networks (HWSNs). The authors of [28] exploited a new optimization algorithm, the physarum optimization, for solving the shortest path problem. This algorithm is with low complexity and high parallelism. Liu et al. [29] applied the percolation theory to solve the exposure-path problem with a two-dimensional (2D) Poisson process in Internet of Things

Using percolation theory to find the critical density of networks could date back to 1961. Gilbert [30] firstly raised the concept of continuum percolation to find the critical density of a Poisson point process. This model is the foundation of wireless networks with continuum percolation. Percolation threshold is also applied to investigate the connectivity of wireless networks. In [31], Penrose indicated that the critical range for the probability of establishing overall connectivity is close to 1, as the number of nodes goes to infinity. This range results in every node connecting to its neighbors on average. Gupta and Kumar of [32] adopted the correlation percolation results to derive the sufficient condition on communication distance for asymptotic connectivity in wireless networks. However, the loose lower and upper bounds on the critical density impose restrictions on the applications of continuumpercolation theory.

Bertin et al. [33] put forward the existence of site and bond percolation for both Poisson and hard-core stationary point processes in the Gabriel graph. Besides, the simulation results demonstrated the critical bounds corresponding to the existence of two paths—open sites and open bounds, respectively. In [34], the authors determined the critical densities of a Poisson point process in different classes of

coverage algorithms. Furthermore, based on the ratio of the connectivity range of base stations to the clients, they showed the almost sure existence of an unbounded connected component. Glauche et al. [35] raised a distributed protocol to guarantee strong connectivity and find the critical communication range of mobile devices in ad hoc networks. An ad hoc network graph could be surely connected above this range. For efficient topology control of wireless networks, Liu and Towsley [36] recommended the concept of monotone percolation based on the local adjustment of communication radii of sensor nodes. Simultaneously, they illuminated some algorithms to guarantee the existence of relatively short paths between any pairs of source and destination nodes. The authors considered both Boolean and probabilistic sensing models to characterize fundamental coverage properties of large-scale sensor networks in [37]. Due to the dependency between coverage and connectivity, Ammari and Das [38] proposed an integrated concentric-sphere model to address coverage and connectivity of 3D WSNs in an integrated way. In [39], through some assumptions and simplifications, Deng et al. gave a simple formula to estimate the minimum number of sensor nodes that the system needed to ensure opportunistic encounter between nodes and made the data forwarded. Khanjary et al. [40] proposed an approach to calculate the density of nodes at critical percolation by using continuum percolation in aligned-orientation directional sensor networks.

However, from the above pieces of literature, we can conclude that most existing percolation-based schemes [34-40] apply the common continuum-percolation theory, enduring the loose lower and upper bounds on the critical density. The tight asymptotic expressions for individual and system outage probabilities are presented in closed form through investigating the performance of time division broadcast (TDBC) protocol in bidirectional cloud networks in the presence of channel estimation errors (CEEs) [41, 42]. To obtain the tighter lower and upper bounds of critical density and make percolation theory more apt to 3D WSNs, we propose a bond-percolation-based scheme that maps the exposure-path prevention problem into a bond-percolation model in a 3D WSN. Depending on the deployment of sensor nodes obeying a 3D Gaussian process, the lower and upper bounds of critical density for 3D omnidirectional WSNs are derived.

3. System Models

Firstly, this section introduces the deployment and sensing models of 3D omnidirectional sensor networks. Then, we adopt the continuum-percolation theory [43] to formulate exposure-path prevention problem. Meanwhile, a bond-percolation scheme is proposed to map the proposed problem into a bond-percolation model.

3.1. System Models

3.1.1. Deployment Model. In a vast 3D WSN, sensor nodes are deployed randomly and their locations are uniformly

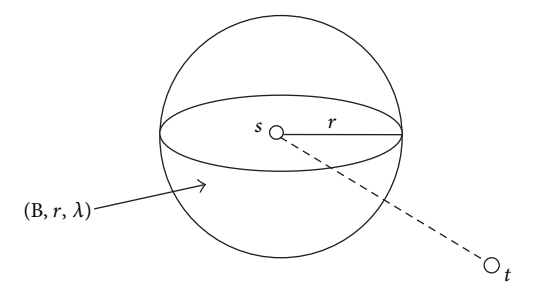


FIGURE 1: Omnidirectional sensing model.

and independently distributed, modeled as a stationary 3D Gaussian distribution [44] with a random variable X and $X \sim N(\mu, \sigma^2)$. μ is the mathematical expectation, that is, the average value. σ represents the standard deviation, and σ^2 denotes the covariance. Then, from [45], we have the probability density function of X; namely,

$$p(X) = \frac{1}{\left(\sqrt{2\pi\sigma^2}\right)^3} \exp\left(-\frac{\left(X - \mu\right)^2}{2\sigma^2}\right). \tag{1}$$

In any subregion V, the number of sensor nodes N(V) = k follows the Gaussian distribution with mean value $\mu = \lambda \|V\|$, where $\|V\|$ is the volume of V. We assume that σ is the standard deviation and σ^2 is the covariance. Therefore, the probability intensity function of N(V') is

$$p(N(V) = k) = \frac{1}{\left(\sqrt{2\pi\sigma^2}\right)^3} \exp\left(-\frac{(k-\lambda \|V\|)^2}{2\sigma^2}\right). \quad (2)$$

3.1.2. Sensing Model. In this paper, we adopt the sphere model (B, r, λ) [16] as the sensing model in a 3D omnidirectional sensor network, as shown in Figure 1. B denotes the node sensing range, a spherical region, and its sensing radius is r. λ is the deployment density of sensor nodes in the 3D WSN. If s: (x_s, y_s, z_s) denote the location of one sensor node, a target point t: (x_t, y_t, z_t) is covered when the Euclidean distance |st| satisfies [38]

$$|st| = \sqrt{(x_s - x_t)^2 + (y_s - y_t)^2 + (z_s - z_t)^2} \le r.$$
 (3)

This paper just considers the omnidirectional sensing model other than the directional sensing model [40]. The directional sensing model in 3D WSNs is the circular cone with one offset angle. Future works of our research focus on the study of the directional sensor network that is more commonly in practice.

3.2. Problem Formulation. In a 3D WSN R^3 , the deployment space is divided into two parts, the vacant region W covered by no sensor node and the covered region C covered by at least one sensor node. The exposure path in a 3D network is defined in the following.

Definition 1 (exposure path). A continuous strip *S* (or curve *S*) from one side to the other side of the deployment region is

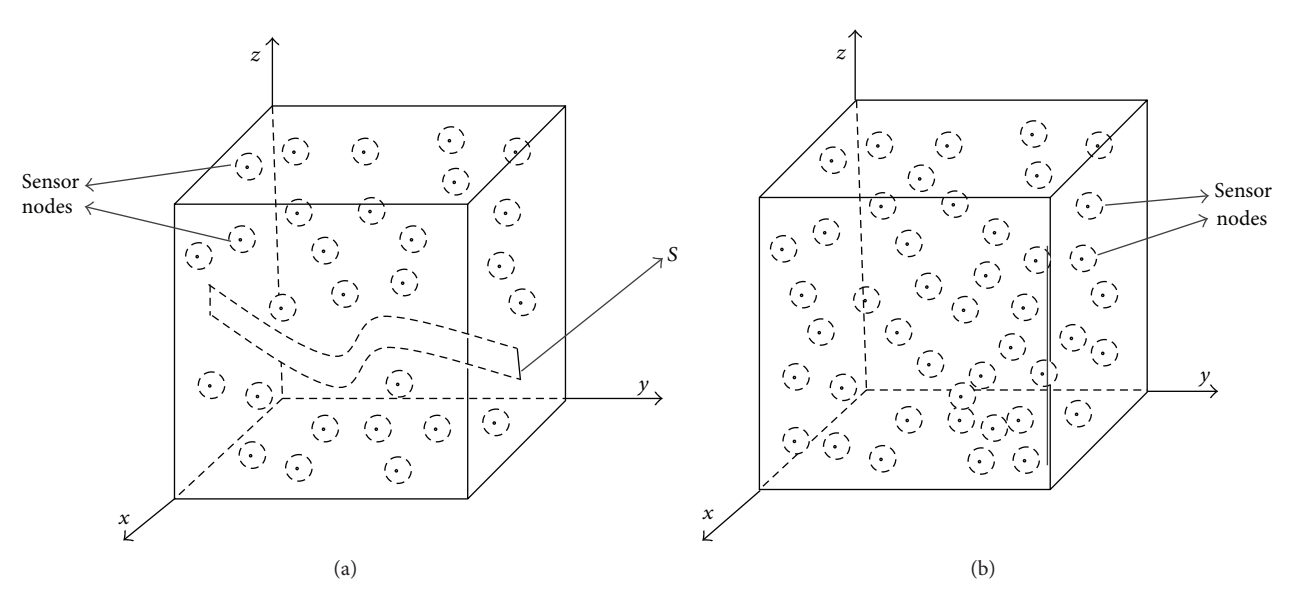


FIGURE 2: Relationship between exposure path S and sensor node density λ_C .

said to be an exposure path if it belongs to any vacant region *W*; see Figure 2(a).

Sensor nodes may be spread in an arbitrary pattern, such as certain sensor deployment strategies, airdropped or launched via artillery in battlefields or unfriendly environments. As shown in Figure 2(a), there exists an exposure path in the 3D network if λ is not larger than the critical threshold λ_C , whereas, in Figure 2(b), if $\lambda > \lambda_C$, no exposure path exists in this network. Additionally, the exorbitant density will cause vast redundancy, high implementation complexity and cost. In conclusion, λ of no exposure paths and no redundancy existing in the network is the optimal density.

As a result, we formulate the exposure-path prevention problem as the calculation of the critical density λ_C in a 3D network. In [46], if the lower and upper bounds of λ_C are very loose, they cannot be applied to determine a practically useful density for nodes deploying process. Concurrently, we summarize from [43] that the bounds on λ_C are very loose, and this scheme of [43] is suitable only for the Poisson model. To get the tighter bounds of λ_C and make the appropriate model in this paper, a bond-percolation model is proposed for the 3D sensor networks based on the bond-percolation theory. We will introduce it in Section 3.3. According to the Limit theory, strip S can be seen as the countless lines superposition. Then, we just consider the condition of lines for simplicity.

3.3. Bond-Percolation Model. In this section, to resolve the exposure-path prevention problem, the 3D sensor network is partitioned into a 3D uniform lattice, as shown in Figure 3. Then, we define the number of lattices in the regions C and W as the sizes of C and W, $d(C,\lambda)$ and $d(W,\lambda)$, respectively. To formulate this problem, the critical densities [13] are defined as $\lambda_C = \inf\{\lambda: p(d(C,\lambda) = \infty) > 0\}$. From the above discussion, it is clear that if $\lambda \leq \lambda_C$, there exists an exposure path in the network.

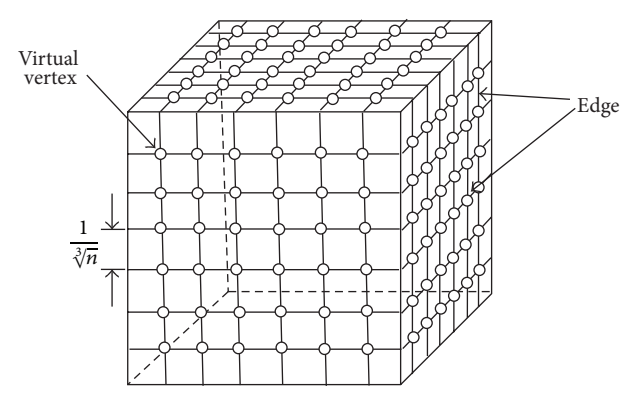


FIGURE 3: The unit cube region with a virtual lattice.

For simplicity, in Figure 3, let one unit cube region contain n vertexes, $M = \{m_1, m_2, \ldots, m_n\}$, and form a $\sqrt[3]{n} \times \sqrt[3]{n}$ lattice. n vertexes do not contain the ones that lie on the edges of this cube. $e_{i,j}$, $i,j \in [1,n]$ denotes the edge between vertex m_i and vertex m_j . Therefore, the length of edge $e_{i,j}$ between neighbor vertexes is $\kappa = 1/\sqrt[3]{n}$. We give the following definitions to identify the relationship between edge $e_{i,j}$ and the bounds of λ_C .

Definition 2 (closed/open edge). For edge $e_{i,j}$, we define two different indicator functions as follows:

$$L\left(e_{i,j}\right)$$

$$=\begin{cases} 1, & \text{if at least one point on } e_{i,j} \text{ is covered;} \\ 0, & \text{if all points on } e_{i,j} \text{ are not covered,} \end{cases} \tag{4}$$

$$U\left(e_{i,j}\right)$$

$$=\begin{cases} 1, & \text{if all points on } e_{i,j} \text{ are covered;} \\ 0, & \text{if at least one point on } e_{i,j} \text{ is not covered.} \end{cases}$$
 (5)

Then, (1) if $L(e_{i,j}) = 1$, $e_{i,j}$ is defined as L-closed edge; if $L(e_{i,j}) = 0$, $e_{i,j}$ is called L-open edge; (2) $e_{i,j}$ is named as U-closed edge if $U(e_{i,j}) = 1$; $e_{i,j}$ is denoted as U-open edge if $U(e_{i,j}) = 0$.

Definition 3 (coverage lattice). In a 3D lattice Z^3 with its vertex set M (|M| = n) and edge set E, if an arbitrary edge $e_{i,j}$ between two neighbor vertexes is L-open/L-closed edge, Z^3 is an L-coverage lattice; if $e_{i,j}$ is U-open/U-closed edge, Z^3 is a U-coverage lattice.

Definition 4 (closed/open path). In a 3D lattice Z^3 with its vertex set M (|M|=n) and edge set E, a path S passes via a sequence of edges $e_{1,2}, e_{2,3}, \ldots, e_{i,i+1}, \ldots, i \geq 1$. If all the edges $(e_{i,i+1}, i \geq 1)$ of path S are L-open/U-open, S is named as the L-open/U-open path; if all the edges are L-closed/U-closed, S is called the L-closed/U-closed path.

According to Definitions 2–4, it is simple to conclude that (a) if edge $e_{i,j}$ is the U-closed edge, it must be the L-closed edge in terms of coverage, and not vice versa; (b) the lower bound λ_L of the critical density λ_C could be derived by L-coverage lattice and the upper bound λ_U by U-coverage lattice for 3D sensor networks.

4. Bounds of Critical Density

In this section, since the probability p of an arbitrary edge in the 3D lattice is closed, there exists a threshold value $p_t \in [0,1]$ resulting in the differences of the global behavior of the system in two regions C and W. Generally speaking, one closed path from one side to the other of the 3D network exists for all $p > p_t$ [47]. Conversely, no closed path exists for all $p < p_t$. For the sake of clearness, we define $P_L = p\{L(e_{i,j}) = 1\}$, $P_U = p\{U(e_{i,j}) = 1\}$; and $\lambda_L = \sup\{\lambda : P_L \le p_t\}$, $\lambda_U = \inf\{\lambda : P_U \ge p_t\}$. Thus, $p\{\text{the exposure path exists}\} > 0$ if $P_L < p_t$, and $p\{\text{the exposure path exists}\} = 0$ if $P_U > p_t$. From [47], we can see that the probabilities of all edges being open or closed are independent in the bond-percolation theory. In Section 4.2, the dependence of P_L (P_U) on neighbor edges will be discussed in 3D omnidirectional sensor networks in detail

4.1. Critical Density λ_C . Firstly, a new operation $A_i \cup A_j = \bigcup_{\forall s_n \in e_{i,j}} A_n$ is defined in this section, where s_n is an arbitrary point on edge $e_{i,j}$ of the L-coverage lattice, and A_n is the sphere centered at s_n with radius r, as shown in Figure 4(a). In the 3D coordinate system, we adopt edge $e_{i,j}$ on y-axis as an example and draw some conclusions. In this figure, m_i and m_j are the two endpoints of edge $e_{i,j}$. Therefore, $A_i \cup A_j$ is a set that contains all the coverage spheres centered at the points of edge $e_{i,j}$. Based on the definition of $A_i \cup A_j$, it is easy to have the following theorem.

Theorem 5. No sensor node within $A_i \cup A_j$ is a sufficient and necessary condition of all points on edge $e_{i,j}$ being not covered by any sensor nodes in the network.

Proof. There are two steps to prove the theorem as follows.

- (1) From the concept of $A_i \cup A_j$ at the start of this section, we know that $A_i \cup A_j$ contains the overall coverage space of all points on $e_{i,j}$. Consequently, it is obvious that if no sensor nodes exist in $A_i \cup A_j$, all points on $e_{i,j}$ are not covered by any sensor nodes.
- (2) On the contrary, if one point on edge e_{i,j} is covered by a sensor node in the network, this sensor node locates within A_i∪A_j on account of the definition of A_i∪A_j. So, obviously, if all points on edge e_{i,j} are not covered by any sensor nodes in the network, there is no sensor node within A_i∪A_j.

To sum up, the proof of Theorem 5 is finished. \Box

Theorem 6. *In a 3D omnidirectional sensor network, we have*

$$\frac{\left\{-2\sigma^{2} \ln \left[\left(2\pi\sigma^{2}\right)^{3/2} \left(1-p_{t}\right)\right]\right\}^{1/2}}{\left(4/3\right)\pi r^{3}+\pi r^{2}\kappa}$$

$$<\lambda_{C} < \frac{\left\{-2\sigma^{2} \ln \left[\left(2\pi\sigma^{2}\right)^{3/2} \left(1-p_{t}\right)\right]\right\}^{1/2}}{\left(2\pi/3\right)\left(2r+\kappa/2\right)\left(r-\kappa/2\right)^{2}},$$
(6)

where $\kappa = 1/\sqrt[3]{n}$.

Proof. There are three processes to demonstrate this theorem. (1) Based on (2), we have

$$p\left\{N\left(A_{i} \cup A_{j}\right) = 0\right\}$$

$$= \frac{1}{\left(\sqrt{2\pi\sigma^{2}}\right)^{3}} \exp\left(-\frac{\left(\lambda \|V\|\right)^{2}}{2\sigma^{2}}\right)$$

$$= \frac{1}{\left(\sqrt{2\pi\sigma^{2}}\right)^{3}} \exp\left(-\frac{\lambda^{2}\left((4/3)\pi r^{3} + \pi r^{2}\kappa\right)^{2}}{2\sigma^{2}}\right),$$
(7)

where $\|V\|$ is the volume of the 3D omnidirectional sensor network, λ is the deployment density of sensor nodes in this network, and $\kappa = 1/\sqrt[3]{n}$. σ^2 is the covariance of the Gaussian distribution, and r is the sensing radius of sensor nodes.

 $-1 - n \{I(e_{ij}) = 0\}$

$$P_{L} = 1 - p \left\{ L\left(e_{i,j}\right) = 0\right\}$$

$$= 1 - \frac{1}{\left(\sqrt{2\pi\sigma^{2}}\right)^{3}} \exp\left(-\frac{\lambda^{2}\left((4/3)\pi r^{3} + \pi r^{2}\kappa\right)^{2}}{2\sigma^{2}}\right).$$
(8)

Therefore, it is clear that P_L increases monotonously as λ increases. Because $\lambda_L = \sup\{\lambda: P_L \leq p_t\}, 1-(1/(\sqrt{2\pi\sigma^2})^3) \exp(-\lambda^2((4/3)\pi r^3 + \pi r^2\kappa)^2/2\sigma^2) = p_t$. As a result, we can get $\lambda_L = \{-2\sigma^2 \ln[(2\pi\sigma^2)^{3/2}(1-p_t)]\}^{1/2}/((4/3)\pi r^3 + \pi r^2\kappa)$ in (6).

(2) By the above analysis, we can know that it is difficult to compute the explicit expression of the probability that

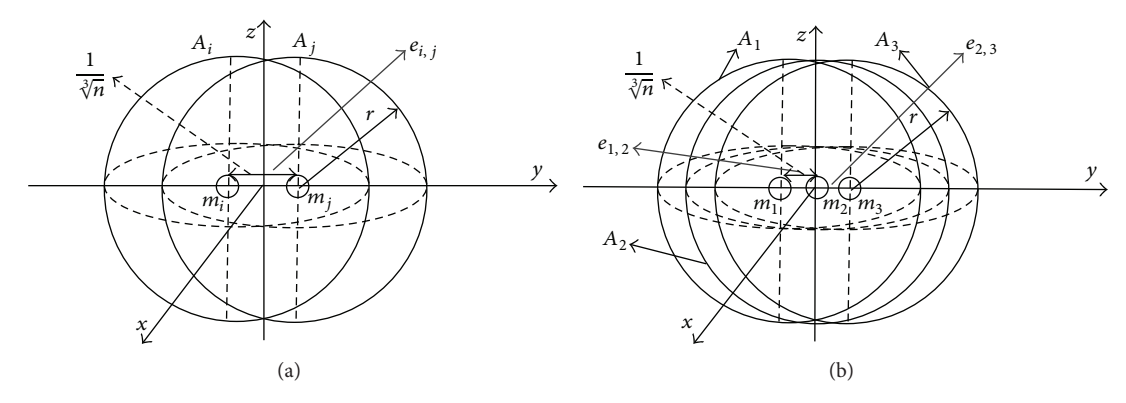


FIGURE 4: Covered region division of the edge $e_{i,j}$.

all points on edge $e_{i,j}$ are covered. Consequently, finding an approximation of P_U is necessary in this paper. We assume P_o is the probability of all points on $e_{i,j}$ being covered by one sensor node, and P_O is the probability of all points on $e_{i,j}$ being covered by one sensor network. According to the definition of P_U and P_O , we have $P_U = P_O > P_o$. Namely,

$$P_U > P\{\text{all points on } e_{i,j} \text{ are covered by one sensor node}\}.$$
(9)

Clearly, one sensor node covers all points on $e_{i,j}$ if and only if some sensor node exists in $A_i \cap A_j$. From (2),

$$p\left\{N\left(A_{i}\bigcap A_{j}\right) > 0\right\}$$

$$= 1 - \frac{1}{\left(\sqrt{2\pi\sigma^{2}}\right)^{3}} \exp\left(-\frac{\lambda^{2} \left\|A_{i}\bigcap A_{j}\right\|^{2}}{2\sigma^{2}}\right). \tag{10}$$

Let the volume of $A_i \cap A_j$ be $||A_i \cap A_j|| = V'$; then in Figure 4(a), we have

$$P_{U} > 1 - \frac{1}{\left(\sqrt{2\pi\sigma^{2}}\right)^{3}}$$

$$\times \exp\left(-\frac{\lambda^{2}\left(\iint_{R} 4\sqrt{r^{2} - \left(x'\right)^{2} - \left(y' - \kappa/2\right)^{2}} d\delta\right)^{2}}{2\sigma^{2}}\right), \tag{11}$$

where (x', y', z') denotes an arbitrary point within $A_i \cap A_j$, $R: (x')^2 + (y')^2 = (r - \kappa/2)^2$, and $d\sigma = dx'dy'$. It is simple to obtain $V' = (2\pi/3)(2r + \kappa/2)(r - \kappa/2)^2$.

In conclusion, we choose P_o as the approximation of P_U in this paper. Let $\lambda_U = \inf\{\lambda: P_o \geq p_t\}$; then $\lambda_U = \{-2\sigma^2 \ln[(2\pi\sigma^2)^{3/2}(1-p_t)]\}^{1/2}/(2\pi/3)(2r+\kappa/2)(r-\kappa/2)^2$ can be achieved in (6).

(3) Equation (5) can be turned into

$$U\left(e_{i,j}\right) = \begin{cases} 1, & \text{if } e_{i,j} \text{ is covered by one sensor node;} \\ 0, & \text{otherwise.} \end{cases}$$

(12)

If $P_L < p_t$, $p\{d(W) = \infty\} > 0$. Let $\lambda_C' = \sup\{\lambda : p\{d(W) = \infty\} > 0\}$; then it is easy to have $\lambda_L < \lambda_C'$. From (10), if $1 - (1/(\sqrt{2\pi\sigma^2})^3) \exp(-(\lambda V')^2/2\sigma^2) > p_t$, $P_U > p_t$. Consequently, $p\{d(C) = \infty\} > 0$. According to the concept of λ_C , $(\{-2\sigma^2 \ln[(\sqrt{2\pi\sigma^2})^3(1-p_t)]\}^{1/2}/V') > \lambda_C$. From (1) and (2), we obtain Theorem 6.

4.2. Dependence among Neighbor Edges. On the basis of (6) and Gaussian distribution, the different values of κ and r can generate the different bounds. The probabilities of all edges $e_{i,j}$ being open or closed are independent in the bond-percolation theory [47]. However, P_L (P_U) of a given edge is dependent on the neighbor edges but independent of most edges in this paper. As a consequence, we can use the bond-percolation model to approximate the coverage percolation in this paper.

In this section, we illustrate the quantitative measure of the dependence between $e_{1,2}$ and $e_{2,3}$ as an example.

(1) Firstly, the mutual information in information theory [48] is employed to measure the mutual dependence between $A = L(e_{1,2})$ and $B = L(e_{2,3})$; that is,

$$I(A, B) = \sum_{a \in \{0,1\}} \sum_{b \in \{0,1\}} P_{AB}(a, b) \log \left(\frac{P_{AB}(a, b)}{P_{A}(a) P_{B}(b)} \right), \quad (13)$$

where $P_{AB}(a,b) = p\{L(e_{1,2}) = a, L(e_{2,3}) = b\}, P_A(a) = p\{L(e_{1,2}) = a\}, \text{ and } P_B(b) = p\{L(e_{2,3}) = b\}.$

In 3D omnidirectional sensor networks, we discuss the mutual dependence between $e_{1,2}$ and $e_{2,3}$, shown in Figure 4(b). I(A, B) reveals the relationships among κ , r and the mutual dependence in this section. From (2), we have

$$\begin{split} P_{A}\left(0\right) &= P_{B}\left(0\right) \\ &= \frac{1}{\left(\sqrt{2\pi\sigma^{2}}\right)^{3}} \exp\left(-\frac{\lambda_{L}^{2}\left(\left(4/3\right)\pi r^{3} + \pi r^{2}\kappa\right)^{2}}{2\sigma^{2}}\right), \end{split} \tag{14}$$

$$P_{A}(1) = P_{B}(1)$$

$$= 1 - \frac{1}{\left(\sqrt{2\pi\sigma^{2}}\right)^{3}} \exp\left(-\frac{\lambda_{L}^{2}\left((4/3)\pi r^{3} + \pi r^{2}\kappa\right)^{2}}{2\sigma^{2}}\right). \tag{15}$$

What is more,

$$P_{AB}(0,0) = p \left\{ N \left(A_1 \cup A_3 \right) = 0 \right\}$$

$$= \frac{1}{\left(\sqrt{2\pi\sigma^2} \right)^3} \exp\left(-\frac{\lambda_L^2 \left((4/3) \pi r^3 + 2\pi r^2 \kappa \right)^2}{2\sigma^2} \right),$$
(16)

$$P_{AB}(1,0) = P_{AB}(0,1)$$

$$= P_{A}(0) - P_{AB}(0,0)$$

$$= \frac{1}{\left(\sqrt{2\pi\sigma^{2}}\right)^{3}}$$

$$\times \left[\exp\left(-\frac{\lambda_{L}^{2}\left((4/3)\pi r^{3} + \pi r^{2}\kappa\right)^{2}}{2\sigma^{2}}\right)\right]$$

$$-\exp\left(-\frac{\lambda_{L}^{2}\left((4/3)\pi r^{3} + 2\pi r^{2}\kappa\right)^{2}}{2\sigma^{2}}\right)\right],$$
(17)

$$P_{AB}(1,1) = 1 - P_{AB}(0,1) - P_{AB}(1,0) - P_{AB}(0,0)$$

$$= 1 + \frac{1}{\left(\sqrt{2\pi\sigma^2}\right)^3}$$

$$\times \left[\exp\left(-\frac{\lambda_L^2\left((4/3)\pi r^3 + 2\pi r^2\kappa\right)^2}{2\sigma^2}\right) - 2\exp\left(-\frac{\lambda_L^2\left((4/3)\pi r^3 + \pi r^2\kappa\right)^2}{2\sigma^2}\right)\right].$$
(18)

Putting these above equations (14)–(18) into (13), we can obtain $I(L(e_{1,2}), L(e_{2,3}))$.

(2) Similarly, the case of $I(U(e_{1,2}), U(e_{2,3}))$ can be achieved in this section. We also adopt the mutual information [48] to measure the mutual dependence between $C = U(e_{1,2})$ and $D = U(e_{2,3})$; namely,

$$I(C, D) = \sum_{c \in \{0,1\}} \sum_{d \in \{0,1\}} P_{CD}(c, d) \log \left(\frac{P_{CD}(c, d)}{P_{C}(c) P_{D}(d)}\right),$$
(19)

where $P_{CD}(c,d) = p\{U(e_{1,2}) = c, U(e_{2,3}) = d\}, P_{C}(c) = p\{U(e_{1,2}) = c\}, \text{ and } P_{D}(d) = p\{U(e_{2,3}) = d\}.$

In Figure 4(b), we use I(C, D) to indicate the relationships among the mutual dependence, κ , and r. Based on

formula (2), we have

$$\begin{split} P_{C}\left(0\right) &= P_{D}\left(0\right) \\ &= 1 - \frac{1}{\left(\sqrt{2\pi\sigma^{2}}\right)^{3}} \\ &\times \exp\left(-\frac{\lambda_{U}^{2}\left(\left(2\pi/3\right)\left(2r + \kappa/2\right)\left(r - \kappa/2\right)^{2}\right)^{2}}{2\sigma^{2}}\right), \end{split}$$

$$(20)$$

$$P_{C}\left(1\right) &= P_{D}\left(1\right) \\ &= \frac{1}{\left(\sqrt{2\pi\sigma^{2}}\right)^{3}} \\ &\times \exp\left(-\frac{\lambda_{U}^{2}\left(\left(2\pi/3\right)\left(2r + \kappa/2\right)\left(r - \kappa/2\right)^{2}\right)^{2}}{2\sigma^{2}}\right). \end{split}$$

Moreover,

 $P_{CD}(1,0)$

$$\begin{split} P_{\text{CD}}(1,1) &= p \left\{ N \left(A_1 \cap A_3 \right) = 0 \right\} \\ &= \frac{1}{\left(\sqrt{2\pi\sigma^2} \right)^3} \\ &\times \exp \left(-\frac{\lambda_U^2 \left((2\pi/3) \left(2r + \kappa \right) (r - \kappa)^2 \right)^2}{2\sigma^2} \right), \end{split} \tag{22}$$

$$= P_{CD}(0,1) = P_{C}(1) - P_{CD}(1,1)$$

$$= \frac{1}{\left(\sqrt{2\pi\sigma^{2}}\right)^{3}}$$

$$\times \left[\exp\left(-\frac{\lambda_{U}^{2}\left((2\pi/3)(2r + \kappa/2)(r - \kappa/2)^{2}\right)^{2}}{2\sigma^{2}}\right) - \exp\left(-\frac{\lambda_{U}^{2}\left((2\pi/3)(2r + \kappa)(r - \kappa)^{2}\right)^{2}}{2\sigma^{2}}\right)\right],$$
(23)

$$\begin{split} P_{CD}(0,0) &= 1 - P_{CD}(0,1) - P_{CD}(1,0) - P_{CD}(1,1) \\ &= 1 + \frac{1}{\left(\sqrt{2\pi\sigma^2}\right)^3} \exp\left(-\frac{\lambda_U^2 \left((2\pi/3)(2r + \kappa)(r - \kappa)^2\right)^2}{2\sigma^2}\right) \\ &- 2\frac{1}{\left(\sqrt{2\pi\sigma^2}\right)^3} \\ &\times \exp\left(-\frac{\lambda_U^2 \left((2\pi/3)(2r + \kappa/2)(r - \kappa/2)^2\right)^2}{2\sigma^2}\right). \end{split}$$

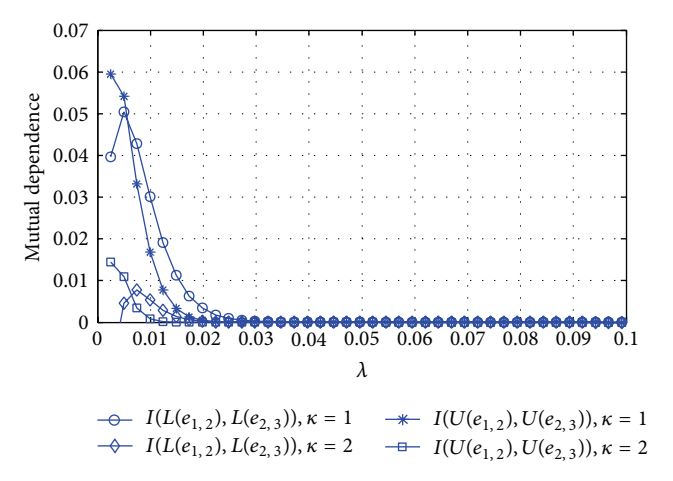


FIGURE 5: Comparison between $I(L(e_{1,2}), L(e_{2,3}))$ and $I(U(e_{1,2}), U(e_{2,3}))$ with different κ .

Putting the formulas (20)–(24) into formula (19), $I(U(e_{1,2}), U(e_{2,3}))$ can be obtained.

(3) Finally, when r=4, $\kappa=1$ or 2, the curves of $I(L(e_{1,2}), L(e_{2,3}))$ and $I(U(e_{1,2}), U(e_{2,3}))$ are depicted in Figure 5. As λ increases, the mutual dependence between neighbor edges decreases and it gets more close to 0. When $\lambda>0.03$, $I(L(e_{1,2}), L(e_{2,3}))$ and $I(U(e_{1,2}), U(e_{2,3}))$ are equal to 0 in this figure. I(A,B)=0 and I(C,D)=0 mean that the two edges are independent of each other [48]. From the observation of this figure, it is tempting to infer that the dependence between neighbor edges is so weak that it can be ignored in this paper. Therefore, we can use the bond-percolation model to approximate the coverage percolation.

5. Simulation Evaluations

In this paper, plentiful simulations are conducted to evaluate the effectiveness and characterize the performance of our models and analytical analyses by MATLAB (version 7.7). In a 3D omnidirectional sensor network, we set the deployment space as a $100 \times 100 \times 100 \,\mathrm{m}^3$ cube and deploy all the homogeneous sensor nodes under a stationary 3D Gaussian process. Based on the covered space of sensor nodes, L-coverage lattice and U-coverage lattice are built, and we analyze the experimental critical densities in the two kinds of lattice, respectively.

Let r=10 and $p_t=0.5$. The number of sensor nodes that we deploy in this network varies from 100 to 1000 per 20 steps. That is to say, the deployment density λ varies from 0.0001 to 0.001 per 0.00002 steps. 50 different (B,r,λ) are randomly generated with each different λ . Let the probability of no exposure path existing be P_N . Then, we obtain three different P_N 's of the continuum percolation, the L-coverage lattice, and the U-coverage lattice for each (B,r,λ) , that is, $P_{N,C}$, $P_{N,L}$, and $P_{N,U}$, respectively.

In the experiments, we calculate the ratio N(closed edges)/N(all edges) for each (B, r, λ) , where N(closed edges) means the number of closed edges and N(all edges) denotes the number of all edges. As a result, 50 ratios for each different

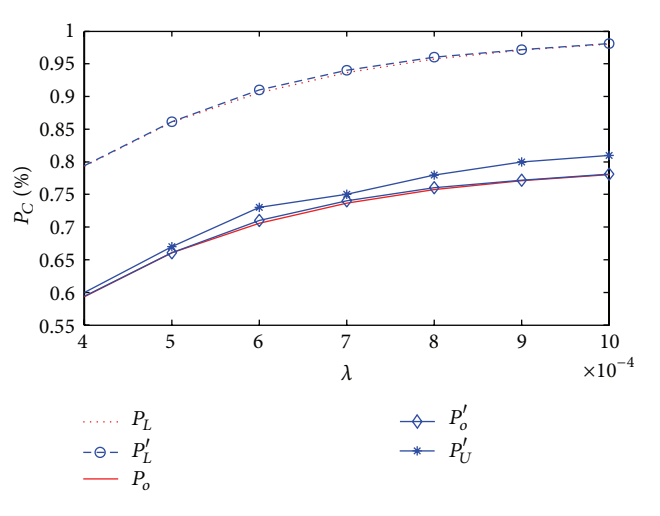


FIGURE 6: Relationship between λ and P_c .

 λ are obtained, which mean the probability P_c of any edge $e_{i,j}$ in the lattice being closed. In Figure 6, we plot the relationship between λ and the probability $P_c = p\{e_{i,j} \text{ is closed}\}$. $P_L = p\{L(e_{i,j}) = 1\}$, and $P_o = p\{\text{all points on } e_{i,j} \text{ are covered by one sensor node}\}$ is an approximation of $P_U = p\{U(e_{i,j}) = 1\}$. P_L and P_o are the analytical values based on Definitions 2–4. P'_L , P'_o , and P'_U are the simulation values in this figure. As λ increases, the analytical values P_L and P_o are more close to the simulation values P'_L and P'_o , respectively. It is clear that P_L and P'_L are larger than P_o and P'_o . Besides, the simulation value P'_U is slightly larger than P'_o and less than P'_L . In consequence, the results of the analytical values very close to the simulation values indicate that our scheme is very effective. Furthermore, we can choose P_o as the approximation of P_U in this paper.

Let r=10 and $\kappa=2$. To get the analytical values, we put the known parameters into formula (6) and obtain the bound 0.00020743 < λ_C < 0.00065816. Meanwhile, the simulation results are $\lambda_L'=0.00020$, $\lambda_U'=0.000580$, and $\lambda_C'=0.000470$. The theoretical values are very close to the simulation values. As shown in Figure 7(a), $P_{N,C}$, $P_{N,L}$, and $P_{N,U}$ increase with the increase of λ , respectively. In conclusion, the simulation results of λ_C are consistent with the analytical results given by Theorem 6.

Similarly, we conduct the experiments with different r and κ and get the corresponding curves of $P_{N,C}$, $P_{N,L}$, and $P_{N,U}$ as shown in Figures 7(b)-7(c). In Figure 7(b), when r=10 and $\kappa=4$, we also substitute the known parameters in formula (6) and get the range 0.00014618 < λ_C < 0.00074137. In the meantime, the simulation results are $\lambda_L'=0.000140$, $\lambda_U'=0.0006310$, and $\lambda_C'=0.000580$, which are consistent with the analytical results shown in Theorem 6. As λ increases, $P_{N,C}$, $P_{N,L}$, and $P_{N,U}$ increase, as shown in this figure.

In Figure 7(c), we set r=15, $\kappa=2$ and put these parameters into formula (6). Then, the bound $0.00015974 < \lambda_C < 0.00037121$ of λ_C is derived based on the theoretical analysis. Simultaneously, the simulation results $\lambda_L'=0.0001490$, $\lambda_U'=0.000370$, and $\lambda_C'=0.000320$ are consistent with the analytical results derived from Theorem 6. What is more, as

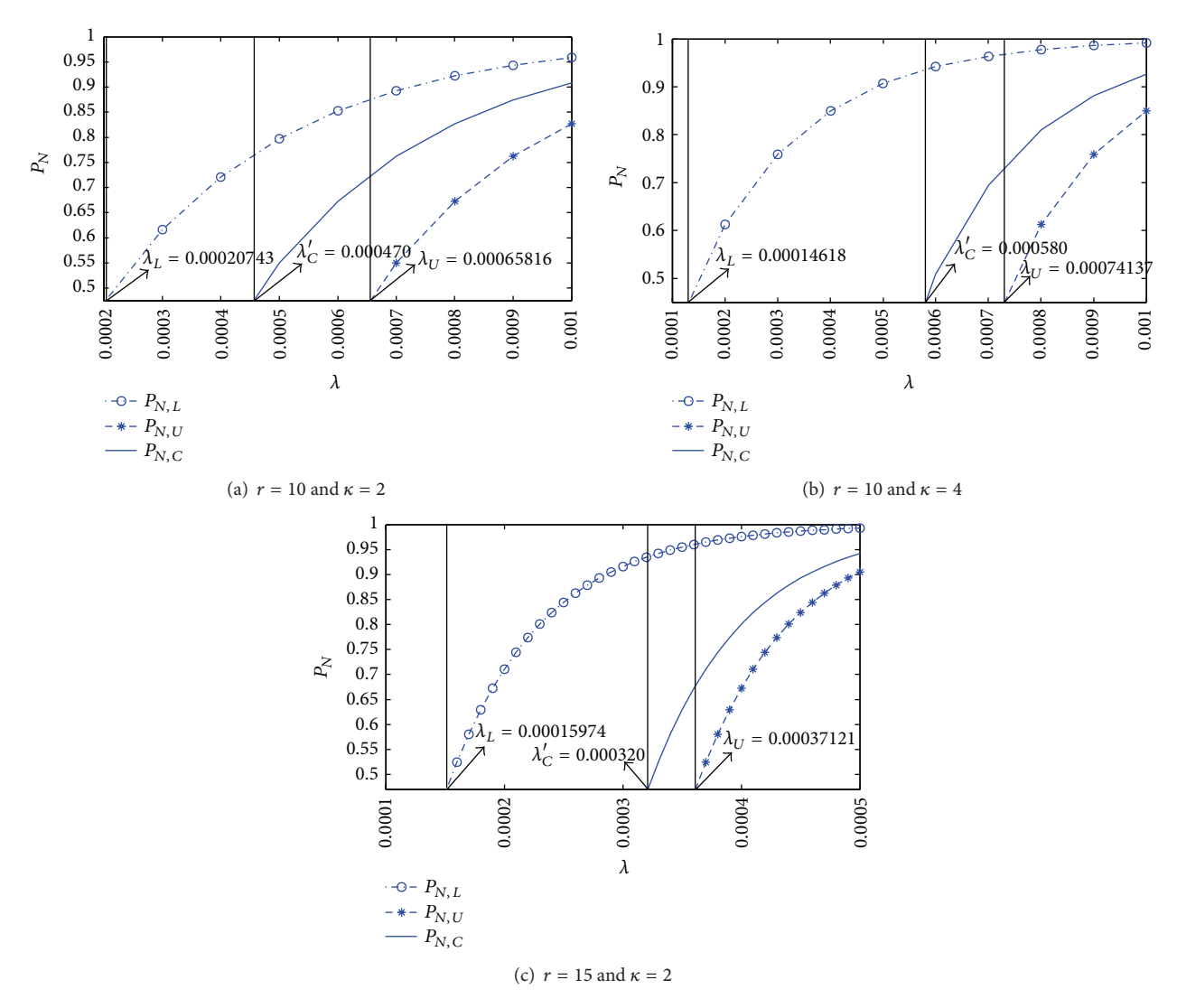


Figure 7: Relationship between P_N and λ with different r and κ .

 λ get larger, $P_{N,C}$, $P_{N,L}$, and $P_{N,U}$ also are in the rising trend.

If the lower and upper bounds of critical density λ_C are very loose, we cannot use them to determine a practically useful density for the network deployment [29]. Generally speaking, all of these above results imply that

- (1) the lower and upper bounds of λ_C become looser as κ increases; that is, the difference between λ_L and λ_U is enhanced as κ increases;
- (2) the lower and upper bounds of λ_C get tighter as r increases; namely, the difference between λ_L and λ_U decreases with the increase of r.

Furthermore, in order to demonstrate the effectiveness of our scheme, we compare the proposed scheme with the existing scheme [16]. For simplicity, we adopt the scheme of [16] into our proposed 3D omnidirectional network model and denote it by CDWMN (critical density of wireless

multihop networks). Our scheme is abbreviated to CDE-PWSN (critical density for exposure-path prevention in wireless sensor networks). When r=10 and $\kappa=2$, Figure 8 compares the lower and upper bounds of critical density between CDWMN and CDEPWSN. In this figure, λ_L and λ_U are the lower and upper bounds of CDEPWSN, while the lower and upper bounds of CDWMN are λ_l and λ_u , respectively. Thus, the corresponding curves are $P_{N,L}$, $P_{N,U}$ and $P_{N,l}$, $P_{N,u}$ of CDEPWSN and CDWMN, respectively.

In Figure 8, we have $\lambda_L = 0.20743 \times 10^{-3}$, $\lambda_U = 0.65816 \times 10^{-3}$, $\lambda_l = 0.1 \times 10^{-3}$, and $\lambda_u = 0.8 \times 10^{-3}$. As λ increases, $P_{N,L}$, $P_{N,U}$ and $P_{N,l}$, $P_{N,u}$ increase. It can be concluded that the lower and upper bounds of critical density, λ_l and λ_u , given by CDWMN are very loose such that we cannot use them to determine a practically useful density for the network deployment. However, the bounds of CDEPWSN are tighter than CDWMN and could be applied to determine a practically useful density for sensor nodes deployment process in 3D WSNs.

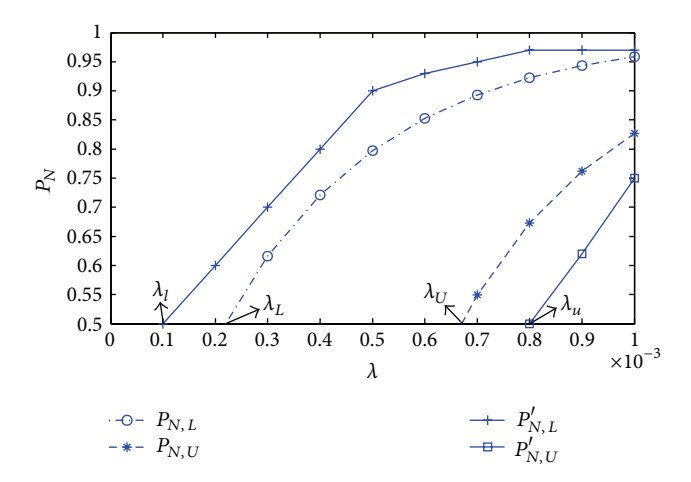


FIGURE 8: Comparison of λ between CDEPWSN and CDWMN with r=10 and $\kappa=2$.

6. Conclusions and Future Works

In this paper, we consider the exposure-path problem that an intruder traverses through a deployment region and the resulting path is not covered by sensor nodes. The network coverage is rather poor if there exists an exposure path in WSNs. To address this problem, we put exposure path into a 3D uniform lattice and propose a bond-percolation-based scheme to calculate the lower and upper bounds of critical density. The proposed models and simulation results show that our scheme can generate reliable and tighter bounds of critical density in 3D wireless sensor networks.

In a practical application, the sensing model of sensor nodes is not omnidirectional but directional. Consequently, our research is still in relatively ideal circumstances. In 3D directional sensor networks, the sensing area of a sensor node is a circular cone, which can be available for consultation in literature [49]. There are lots of difficulties to study the exposure-path prevention in a directional sensing model, such as the setting conditions, distributions, and multifarious calculation. However, this study has a practical significance. Based on the existing works, our future work is to solve the exposure-path prevention in 3D directional sensor networks.

Conflict of Interests

The authors declare that there is no conflict of interests regarding the publication of this paper.

Acknowledgments

This work is supported by the Important National Science & Technology Specific Projects of the Ministry of Science and Technology of China (no. 2013ZX03006001) and New Century Excellent Talents in University (NCET) (no. NCET-11-0593), the National High Technology Research and Development Program of China ("863" Program, no.

SQ2015AA0102085), and the National Natural Science Foundation of China (no. NSFC61471064). The authors also gratefully acknowledge the helpful comments and suggestions of the anonymous reviewers.

References

- [1] S. Guo, H. Zhang, Z. Zhong, J. Chen, Q. Cao, and T. He, "Detecting faulty nodes with data errors for wireless sensor networks," *ACM Transactions on Sensor Networks*, vol. 10, no. 3, article 40, 2014.
- [2] X. M. Jia and C. C. Zheng, "A wireless sensor network node coverage discriminant model based on the average distance of neighbor node," *Applied Mechanics and Materials*, vol. 519, pp. 1264–1270, 2014.
- [3] B. Wang, "Coverage problems in sensor networks: a survey," *ACM Computing Surveys*, vol. 43, article 32, 2011.
- [4] Q. Yang, S. He, J. Li, J. Chen, and Y. Sun, "Energy-efficient probabilistic area coverage in wireless sensor networks," *IEEE Transactions on Vehicular Technology*, 2014.
- [5] S. He, J. Chen, J. Li, and Y. Sun, "Introduction to area coverage in sensor networks," in *Energy-Efficient Area Coverage for Intruder Detection in Sensor Networks*, Springer Briefs in Computer Science, pp. 1–10, Springer, New York, NY, USA, 2014.
- [6] Y. Wang, W. Fu, and D. P. Agrawal, "Gaussian versus uniform distribution for intrusion detection in wireless sensor networks," *IEEE Transactions on Parallel and Distributed Systems*, vol. 24, no. 2, pp. 342–355, 2013.
- [7] G. J. Fan and S. Y. Jin, "Coverage problem in wireless sensor network: a survey," *Journal of Networks*, vol. 5, no. 9, pp. 1033– 1040, 2010.
- [8] G. Vermeeren, W. Joseph, and L. Martens, "Statistical multipath exposure method for assessing the whole-body SAR in a heterogeneous human body model in a realistic environment," *Bioelectromagnetics*, vol. 34, no. 3, pp. 240–251, 2013.
- [9] H. Kesten, Percolation Theory for Mathematicians, Birkhauser, Boston, Mass, USA, 1982.
- [10] G. Grimmett, What is Percolation? Springer, New York, NY, USA, 2nd edition, 1999.
- [11] A. Hunt, R. Ewing, and B. Ghanbarian, Percolation Theory for Flow in Porous Media, vol. 880 of Lecture Notes in Physics, 2014.
- [12] S. R. Broadbent and J. M. Hammersley, "Percolation processes. I. Crystals and mazes," *Proceedings of the Cambridge Philosophical Society*, vol. 53, no. 3, pp. 629–641, 1957.
- [13] D. Stauffer and A. Aharony, *Introduction to Percolation Theory*, Taylor & Francis, London, UK, 1991.
- [14] F. Xing and W. Wang, "On the critical phase transition time of wireless multi-hop networks with random failures," in *Proceedings of the 14th ACM International Conference on Mobile Computing and Networking (MOBICOM '08)*, pp. 175–186, 2008.
- [15] S. Mertens and C. Moore, "Continuum percolation thresholds in two dimensions," *Physical Review E—Statistical, Nonlinear,* and Soft Matter Physics, vol. 86, no. 6, Article ID 061109, 2012.
- [16] S. C. Ng, G. Mao, and B. D. O. Anderson, "Critical density for connectivity in 2D and 3D wireless multi-hop networks," *IEEE Transactions on Wireless Communications*, vol. 12, no. 4, pp. 1512–1523, 2013.
- [17] J. Liang, M. Liu, and X. Kui, "A survey of coverage problems in wireless sensor networks," *Sensors & Transducers Journal*, vol. 163, no. 1, pp. 240–246, 2014.

- [18] X. Li, G. Fletcher, A. Nayak, and I. Stojmenovic, "Placing sensors for area coverage in a complex environment by a team of robots," ACM Transactions on Sensor Networks, vol. 11, no. 1, article 3, 2014.
- [19] S. He, J. Chen, X. Li, X. S. Shen, and Y. Sun, "Mobility and intruder prior information improving the barrier coverage of sparse sensor networks," *IEEE Transactions on Mobile Comput*ing, vol. 13, no. 6, pp. 1268–1282, 2014.
- [20] P. Ostovari, M. Dehghan, and J. Wu, "Connected point coverage in wireless sensor networks using robust spanning trees," in Proceedings of the 31st International Conference on Distributed Computing Systems Workshops (ICDCSW '11), pp. 287–293, June 2011.
- [21] S. Meguerdichian, F. Koushanfar, G. Qu, and M. Potkonjak, "Exposure in wireless ad-hoc sensor networks," in *Proceedings* of the 7th Annual International Conference on Mobile Computing and Networking, pp. 139–150, ACM, July 2001.
- [22] S. Megerian, F. Koushanfar, G. Qu, G. Veltri, and M. Potkonjak, "Exposure in wireless sensor networks: theory and practical solutions," *Wireless Networks*, vol. 8, no. 5, pp. 443–454, 2002.
- [23] G. Veltri, G. Qu, Q. Huang, and M. Potkonjak, "Minimal and maximal exposure path algorithms for wireless embedded sensor networks," in *Proceedings of the 1st International Conference* on Embedded Networked Sensor Systems (SenSys '03), pp. 40–50, ACM, November 2003.
- [24] B. Wang, C. K. Chua, and W. Wang, "Worst and best information exposure paths in wireless sensor networks," in *Mobile Ad-Hoc and Sensor Networks*, pp. 52–62, Springer, Berlin, Germany, 2005.
- [25] H. Djidjev, "Efficient computation of minimum exposure paths in a sensor network field," in *Proceedings of the International Conference on Distributed Computing in Sensor Systems (DCOSS '07)*, vol. 4549 of *Lecture Notes in Computer Science*, pp. 295–308, February 2007.
- [26] H. Djidjev, "Approximation algorithms for computing minimum exposure paths in a sensor field," ACM Transactions on Sensor Networks, vol. 7, no. 3, pp. 1–3, 2010.
- [27] S. Ferrari and G. Foderaro, "A potential field approach to finding minimum-exposure paths in wireless sensor networks," in *Proceedings of the IEEE International Conference on Robotics* and Automation (ICRA '10), pp. 335–341, Anchorage, Alaska, USA, May 2010.
- [28] L. Liu, Y. Song, H. Ma, and X. Zhang, "Physarum optimization: a biology-inspired algorithm for minimal exposure path problem in wireless sensor networks," in *Proceedings of the IEEE Conference on Computer Communications (INFOCOM '12)*, pp. 1296–1304, Orlando, Fla, USA, March 2012.
- [29] L. Liu, X. Zhang, and H. Ma, "Percolation theory-based exposure-path prevention for wireless sensor networks coverage in internet of things," *IEEE Sensors Journal*, vol. 13, no. 10, pp. 3625–3636, 2013.
- [30] E. N. Gilbert, "Random plane networks," Journal of the Society for Industrial and Applied Mathematics, vol. 9, no. 4, pp. 533– 543, 1961.
- [31] M. D. Penrose, "The longest edge of the random minimal spanning tree," *The Annals of Applied Probability*, vol. 7, no. 2, pp. 340–361, 1997.
- [32] P. Gupta and P. R. Kumar, "Critical power for asymptotic connectivity in wireless networks," in *Proceedings of the Stochastic*

- Analysis, Control, Optimization and Applications, pp. 657–566, 1998
- [33] E. Bertin, J.-M. Billiot, and R. Drouilhet, "Continuum percolation in the Gabriel graph," *Advances in Applied Probability*, vol. 34, no. 4, pp. 689–701, 2002.
- [34] L. Booth, J. Bruck, M. Franceschetti, and R. Meester, "Covering algorithms, continuum percolation and the geometry of wireless networks," *The Annals of Applied Probability*, vol. 13, no. 2, pp. 722–741, 2003.
- [35] I. Glauche, W. Krause, R. Sollacher, and M. Greiner, "Continuum percolation of wireless ad hoc communication networks," *Physica A: Statistical Mechanics and Its Applications*, vol. 325, no. 3-4, pp. 577–600, 2003.
- [36] B. Liu and D. Towsley, "A study of the coverage of large-scale sensor networks," in *Proceedings of the IEEE International Conference on Mobile Ad-Hoc and Sensor Systems (MASS '04)*, pp. 475–483, October 2004.
- [37] A. Jiang and J. Bruck, "Monotone percolation and the topology control of wireless networks," in *Proceedings of the 24th Annual Joint Conference of the IEEE Computer and Communications* (INFOCOM '05), pp. 327–338, March 2005.
- [38] H. M. Ammari and S. K. Das, "Critical density for coverage and connectivity in three-dimensional wireless sensor networks using continuum percolation," *IEEE Transactions on Parallel* and Distributed Systems, vol. 20, no. 6, pp. 872–885, 2009.
- [39] Y. Deng, S. Wu, S. Li, Y. Xiong, and T. Zhang, "Lower bound estimation for required number of nodes in the opportunistic communication—based wireless sensor network," in *Advanced* in Computer Science and Its Applications, vol. 279 of Lecture Notes in Electrical Engineering, pp. 869–875, Springer, Berlin, Germany, 2014.
- [40] M. Khanjary, M. Sabaei, and M. R. Meybodi, "Critical density for coverage and connectivity in two-dimensional alignedorientation directional sensor networks using continuum percolation," *IEEE Sensors Journal*, vol. 14, no. 8, pp. 2856–2863, 2014.
- [41] M. Wu, J. Li, J. Ge, C. Zhang, and F. Pop, "Impact of channel estimation error on time division broadcast protocol in bidirectional relaying systems," in *Proceedings of the 5th IEEE International Conference on Intelligent Networking and Collaborative Systems (INCoS '13)*, pp. 348–352, Xi'an, China, September 2013.
- [42] J. Li, M. Wu, J. Ge, C. Zhang, F. Pop, and Y. Wang, "Performance analysis of bidirectional cloud networks with imperfect channel state information," *Concurrency and Computation: Practice and Experience*, 2014.
- [43] R. Meester and R. Roy, *Continuum Percolation*, Cambridge University Press, Cambridge, UK, 1996.
- [44] Y. Shiota, T. Nozaki, F. Bonell, S. Murakami, T. Shinjo, and Y. Suzuki, "Induction of coherent magnetization switching in a few atomic layers of FeCo using voltage pulses," *Nature Materials*, vol. 11, no. 1, pp. 39–43, 2012.
- [45] J.-J. Greffet and C. Baylard, "Nonspecular astigmatic reflection of a 3D gaussian beam on an interface," *Optics Communications*, vol. 93, no. 5-6, pp. 271–276, 1992.
- [46] P. Hall, "On continuum percolation," The Annals of Probability, vol. 13, no. 4, pp. 1250–1266, 1985.
- [47] H. Kesten, "The critical probability of bond percolation on the square lattice equals 1/2," *Communications in Mathematical Physics*, vol. 74, no. 1, pp. 41–59, 1980.

- [48] T. M. Cover and J. A. Thomas, *Elements of Information Theory*, John Wiley & Sons, New York, NY, USA, 2012.
- [49] H. Ma, X. Zhang, and A. Ming, "A coverage-enhancing method for 3d directional sensor networks," in *Proceedings of the IEEE Conference on Computer Communications (INFOCOM '09)*, pp. 2791–2795, IEEE, 2009.